THESIS

ASSESSMENT OF FINE PARTICLES EMITTED FROM PAPER PRINTING AND SHREDDING PROCESSES

Submitted by

Nara Shin

Department of Environmental and Radiological Health Sciences

In partial fulfillment of the requirements

For the Degree of Master of Science

Colorado State University

Fort Collins, Colorado

Spring 2019

Master's Committee:

Advisor: Candace Su-Jung Tsai

Stephen Reynolds
Tiezheng Tong

ABSTRACT

ASSESSMENT TO FINE PARTICLES EMITTED

DURING PAPER PRINTING AND SHREDDING PROCESSES

In this study, we investigated the airborne particles released during paper printing and paper shredding processes in an attempt to characterize and differentiate these particles. Particle characteristics were studied with real-time instruments (RTI) to measure concentrations and with samplers to collect particles for subsequent microscopy and cytotoxicity analysis. The particles released by paper shredding were evaluated for cytotoxicity by using *in vitro* human lung epithelial cell models. A substantial amount of particles were released during both the shredding and printing processes. We found that the printing process caused substantial release of particles with sizes of less than 300 nm in the form of metal granules and graphite. These released particles contained various elements including Al, Ca, Cu, Fe, Mg, N, K, P, S, and Si. The particles released by the paper shredding processes were primarily nanoparticles and had a peak size between 27.4 nm and 36.5 nm. These paper particles contained elements including Al, Br Ca, Cl, Cr, Cu, Fe, Mg, N, Na, Ni P, S, and Si, as determined by scanning electron microscope-energy dispersive X-ray spectroscopy (SEM-EDS) and single-particle inductively coupled plasma-mass spectroscopy (SP-ICP-MS) analysis. Although various metals were identified in the paper particles, these particles did not elicit cytotoxicity to simian virus-transformed bronchial epithelial cells (BEAS2B) and immortalized normal human bronchial epithelial cells (HBE1). However, future studies should investigate other cytotoxicity effects of these paper particles in various types of lung cells to identify potential health effects of the particles.

TABLE OF CONTENTS

ABSTRACT ... ii

ACKNOWLEDGEMENTS ... v

LIST OF TABLES ... vii

LIST OF FIGURES ... viii

CHAPTER 1: INTRODUCTION ... 1

CHAPTER 2: MATERIALS AND METHODS ... 3

2.1) PRINTER EMISSION TEST ... 4

2.2) PAPER PARTICLES EMITTED FROM SHREDDING ACTIVITIES ... 8

2.3) MICROSCOPY ANALYSIS ... 9

2.4) IN VITRO CYTOTOXICITY ASSAYS OF PAPER PARTICLES RELEASED BY SHREDDING ACTIVITIES ... 9

2.4.1) GENERATION AND COLLECTION OF PAPER PARTICLES FOR CYTOTOXICITY ASSAYS ... 9

2.4.2) PREPARATION FOR CYTOTOXICITY ASSAYS ... 10

2.4.3) IN VITRO CYTOTOXICITY ASSAYS ... 11

2.4.4) STATISTICAL ANALYSIS ... 12

2.5) SP-ICP-MS ANALYSIS ... 12

CHAPTER 3: RESULTS AND DISCUSSION ... 14

3.1) PRINTER EMISSION TESTS 14

3.2) MORPHOLOGY AND ELEMENTAL COMPOSITION ANALYSIS OF PRINTER EMISSIONS 18

3.3) PAPER PARTICLES EMITTED FROM SHREDDING ACTIVITIES 23

3.4) ANALYSIS OF PAPER SURFACE AND ELEMENTAL COMPOSITION 26

3.5) CYTOTOXICITY EFFECTS OF RELEASED PAPER PARTICLES AND ELEMENTAL COMPOSITION ANALYSIS 28

CHAPTER 4: CONCLUSIONS 32

REFERENCES 33

APPENDIX A: LIST OF TABLES 38

ACKNOWLEDGEMENTS

This study is based on the research conducted on nano- to micro- sized particles released from printer usage and paper shredding activities. I am grateful for a number of people including my family, friends and colleagues for their encouragement on the research, support and publication.

First, I am especially grateful to my family, Yong-Gi Shin (Dad), In-Seon Song (Mom), DaeYong Shin, and JuYong Shin who supported me always. I always knew that you believed in me and wanted the best for me. Thank you for guiding me to grow as a strong and independent woman over last 10 years in the United States.

I would like to express my sincere gratitude to my advisor Dr. Candace Su-Jung Tsai, *Senior Assistant Professor of Industrial Hygiene and Environmental Health, Colorado State University*, who truly believed me and enhanced my active involvement throughout the years. I wouldn't be able to get into this field without your support and guidance throughout my journey.

I would also like to thank my all committee members, Dr. Stephen Reynolds, *Professor and Associate Head of Department of Environmental and Radiological Health Sciences, Colorado State University* and Dr. Tiezheng Tong, *Assistant Professor, Department of Civil and Environmental Engineering, Colorado State University*, for their candid guidance and continuous support during the accomplishment of study.

Finally, I am extremely thankful to Dr. Alison Bauer, Assistant Professor, Department of Environmental and Occupational Health, University of Colorado Denver Anschutz Medical Campus, and Dr. Kalpana Velmurugan, Senior Professional Research Assistant, Dr. Bauer's Lab, University of Colorado Denver Anschutz Medical Campus, for their valuable and professional support on every stage of cytotoxicity.

I further extend my gratitude to Dr. Roy Geiss for technical support on TEM and EDS analysis and Dr. Jacqueline Chaparro for technical analysis on SP-ICP-MS.

This research is funded by Education and Research Center (Grant #T42/OH008432-09) and Centers for Disease Control and Prevention (Grant #T42/OH0092-29). The contents are solely the responsibility of the authors and do not necessarily represent the official views of the Centers for Disease Control and Prevention or the Department of Health and Human Services.

LIST OF TABLES

Table 1. Average total concentrations from printer particle release tests, as measured by NanoScan SMPS and OPS.. 14

Table 2. Average particle concentrations of one-half fractions of each experiment during shredding only by particle size 25

Table 3. Average total concentration from shredding experiments, as measured by NanoScan SMPS and OPS.. 26

LIST OF FIGURES

Figure 1. Illustration of the emission test experimental setup. (a) Front view of the printer emission experiment setup. (b) Top view of the shredding experiment setup. (c) Three-dimensional view of the shredding experiment setup. 5

Figure 2. Real time instrument (RTI) data for emission tests from running 1,000 plain paper sheets and printing 1,000 sheets. (a)-(c) Total concentrations from three repeated experiments running 1,000 sheets each, as measured by RTIs. (d)-(f) Total concentrations from three repeated experiments printing 1,000 sheets each, as measured by RTIs. 7

Figure 3. NanoScan SMPS data of emitted particle size distribution. (a) Average particle size distributions of three repeated experiments running 1,000 sheets each, as represented in Fig. 2a–2c. (b) Average particle size distributions of three repeated experiments printing 1,000 sheets each, as represented in Fig. 2d–2f. 16

Figure 4. Real time instrument (RTI) data of emission tests from running 1,000 plain paper sheets and printing 1,000 sheets. (a) Particle size distribution for running 1,000 plain sheets, as determined by OPS (0.3–10 μm). (b) Particle size distribution for printing 1,000 sheets, as determined by OPS. 17

Figure 5. Microscopy analysis (SEM/TEM/EDS) of printer emitted particles. (a) SEM image of printer emitted particles on a TDS polycarbonate filter. (b) TEM image showing collected printer emitted particles on a TDS copper grid at low magnification. (c) TDS TEM image of printer emitted particles, with many attached granular particles, at high magnification. (d) TEM-EDS image of analyzed particles with attached granules, as observed through TDS. (e) EDS quantitative analysis of the image in (d) and qualitative analysis indicated by color. 18

Figure 6. Microscopic analysis (TEM) of printer emitted particles collected on a TDS Cu grid. Various shapes of particles were observed. 19

Figure 7. Graphite TEM lattice analysis. (a) Representative TEM image of graphite particles emitted from the printer (b) The intensity line profile of the selected area from (a). 19

Figure 8. Printer emission particle analysis via EDS, showing granules attached in one particle, as determined using TDS. 21

Figure 9. RTI [OPS (0.3–10 μm) and SMPS (10–420 nm)] data for shredding 40 sheets of plain and printed paper. (a) Area total particle concentration, as measured by RTIs. (b) Paper particle size distribution, as determined by NanoScan SMPS. (c) Paper particle size distribution, as determined by OPS. 24

Figure 10. Paper particles observed from the shredding process. Various shapes of particles were observed through TEM. 27

Figure 11. Microscopy analysis of paper particles from shredding plain and printed paper. (a) SEM images of plain paper at low and high magnification. (b) EDS quantitative and qualitative analyses of image (a), plain paper. (c) SEM images of printed paper at low and high magnification. (d) EDS quantitative and quantitative analysis of image (c), printed paper. 28

Figure 12. Cell viabilities in two different cell lines (BEAS2B and HBE1) after paper particle exposure for 24-48 h. The mean values of each concentration are presented in bar graphs as a percentage with respect to the control in each cell line not exposed to paper particles. Error bars are standard error of the mean. (a) Changes in viability in the BEAS2B cell line. (b) Changes in viability in the HBE1 cell line. 29

Figure 13. Average element intensities of paper particles in media used for cytotoxicity assays, with standard error bars of each mean measured by SP-ICP-MS, representing the net intensity difference after subtraction of the blank sample. (a) Overall intensity results in a scale up to 15,000 μg/g. (b) Intensity results in a scale less than 700 μg/g of the highlighted area in (a). 31

CHAPTER 1

INTRODUCTION

Many employees work 8 h per day, and some spend more than one-third of the day in various indoor settings such as manufacturing industries, offices and laboratories in the workplace. However, most workers are not aware of either the indoor air quality or their potential exposure to hazardous substances in the workplace. Indoor air quality depends on various factors, such as the frequency of contaminant release, the type and amount of particles emitted from equipment use, the air ventilation exchange rate and the intake air quality[1-3]. Over the past decade, indoor air quality issues have increasingly raised concerns, and some studies have reported potential causes of indoor air quality issues and their consequent health effects[3-7]. With accelerated development of technology, printers are now became commonplace at home and workplace. Karrasch et al. have investigated the effects of laser printer device emissions on human subjects in low-level and high-level exposures and have reported 15 symptoms related to laser printer emission in 37 subjects[6]. Many factors contribute to particle release, especially from printers; these factors include the temperature, speed of printing, toner components and fuser[8, 9]. Bai et al addressed that toner, the potential major source of printer particle emission, consists of various components, such as thermoplastic polymers and styrene-acrylate copolymers, which are fixed onto the paper in a process called 'fusing' during printing[10]. On the basis of this known information, toxicological studies were done using bronchoalveolar lavage fluids (BALF) cells and alveolar macrophages in mice exposed to toner particles. An increase in total BALF cell number and a decrease in body weight have been observed during the recovery phase (9, 28, 56, and 84 days) after exposure in mouse models[10]. Pirela et al. have shown that exposure to printer emitted particles elicits biological responses in human cell lines, such as substantial damage to membrane integrity and increased release of pro-inflammatory cytokines[11].

Tsai et al. have investigated the airborne particles emitted inside the shredder basket during paper shredding[12]. A substantial amount of particles containing various elements such as C, Pt, Si and Ca, and ranging in sizes from nanometers to micrometers, were found inside the shredder.

Although those scientific studies above have indicated that exposure to printer emission causes self-reported symptoms and biological responses from animal and human cell lines, characteristics of the printer emitted particles, as well as the paper utilized printer emitted particles haven't been addressed yet[6, 10-13]. The characteristics of particles may play a role on respiratory related symptoms of current heavy printer and shredder use on indoor air quality [1, 6, 7, 10-17]. The potential health effects from toxicity of particles and exposure levels have not yet attracted sufficient public attention to support further investigation. This research aimed to characterize the particles released from printing and shredding of plain and printed paper, and to investigate the potential toxicity of the emitted paper particles by using *in vitro* cytotoxicity assays.

CHAPTER 2

MATERIALS AND METHODS

The study comprised four parts: (1) evaluation of printer particle release, (2) evaluation of particle release from the shredding of plain and printed paper, (3) microscopy analysis of the released particles and (4) evaluation of the *in vitro* cytotoxicity of paper particles released during shredding.

Equipment

Direct reading real time instruments (RTIs), including a NanoScan scanning mobility particle sizer (NanoScan SMPS) (model 3910, TSI, Shoreview, MN, USA) and an optical particle sizer (OPS) (model 3330, TSI, Shoreview, MN, USA) were used in this study. The NanoScan SMPS measures particle size ranges of 10–420 nm, as monitored in NanoScan manager software (version 1.0.0.19). The OPS measures a particle size range of 0.3–10 µm, as monitored in aerosol instrument manager software (version 9.0.0.0). Both instruments recorded data with a 1 min response time; the NanoScan SMPS was operated at a flow rate of 0.9 L/min, and the OPS was operated at a flow rate of 1.0 L/min.

Two nanoparticle samplers were used to collect the released particles. A Tsai diffusion sampler (TDS) was used to collect particles in the respirable and nanometer size ranges[18]. The TDS uses a transmission electron microscopy (TEM) copper grid (400-mesh with SiO_2 film coating, SPI, West Chester, PA, USA) attached to the center of a 25 mm-diameter polycarbonate membrane filter (0.22 µm pore size, Millipore, Billerica, MA, USA) as the sampling substrate to collect particles and it was operated at a flow rate of 0.3 L/min[18]. One polycarbonate filter and one TEM grid were used to sample particles for each experiment.

2.1) Printer Emission Test

Experiments were conducted in a NanoHood (Labconco, Kansas City, MO, USA). The high-efficiency particulate air (HEPA) filtration of the NanoHood was always in operation during the experiments. The atmospheric temperature and relative humidity during each experiment were measured with a VeloCalc air velocity meter (model 9515, TSI, Shoreview, MN, USA); the average relative humidity was approximately 51.3%, and the average temperature was 20–21 °C.

Particle release tests were conducted to assess the release and its constituents related to the toner use (TN420, Brother, Bridgewater, NJ, USA) during paper printing. The printer exhaust fan (D06K-24TU, Nidec Corporation, St. Louis, MO, USA) fixed in a monochrome laser printer (HL-2270DW, Brother, Bridgewater, NJ, USA) had a maximum air flow rate of 0.63 m^3/min. The same monochrome laser printer, toner, and paper (multipurpose copy paper, 8 ½" x 11", #513096, Staples, Framingham, MA, USA) were used for all experiments. Particle release was studied during the printing 1,000 sheets of paper and was compared with the release in control experiments, running 1,000 blank sheets of paper. To improve measurements, a custom-made hood compartment was attached to the printer exhaust port, as shown in Fig. 1a, to contain the released particles within the hood space for consistent measurement and collection in each experiment. The hood was an approximately 160° angled cone hood with a 0.115 m (4.5 in) inlet diameter, 0.305 m (12 in) outlet diameter and 0.18 m (7 in) duct length. The measurements were taken approximately 0.14 m horizontally from the center of the printer exhaust port, and the average air velocity at this sampling location was approximately 0.3 m/sec. The entire surface of the hood was wiped with isopropyl alcohol before and after each experiment.

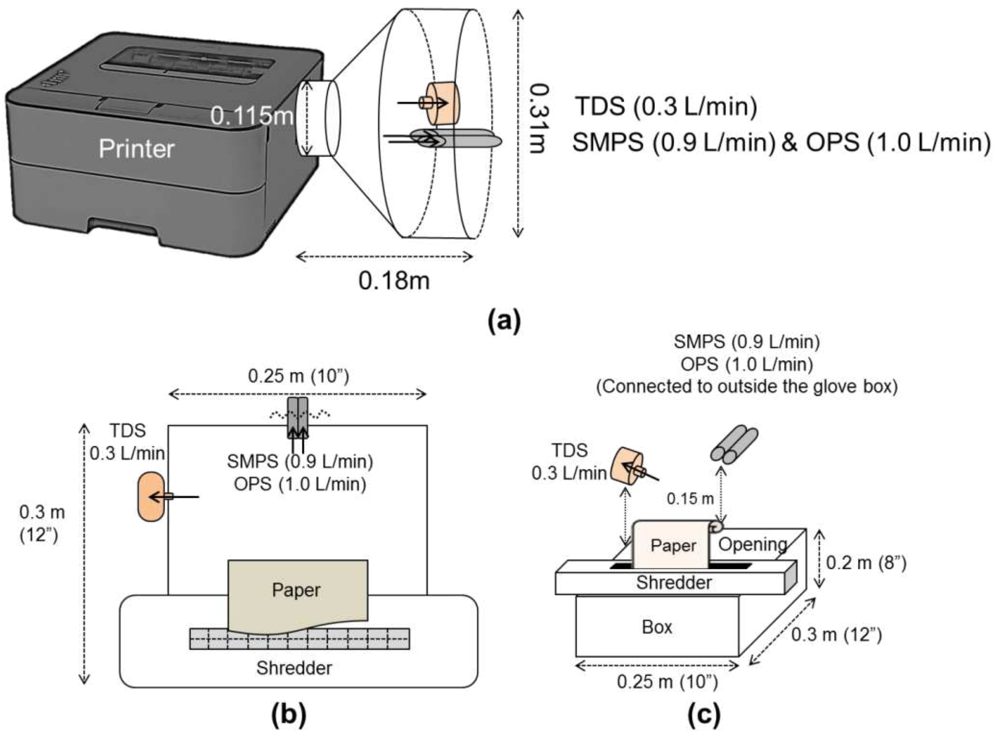

Figure 1. Illustration of the emission test experimental setup. (a) Front view of the printer emission experiment setup. (b) Top view of the shredding experiment setup. (c) Three-dimensional view of the shredding experiment setup.

Tubing 0.45 m in length (Tygon, Saint-Gobin, Malvern, PA, USA) was connected to the RTIs and between the sampling pump and TDS to reach the sampling location at the center of the custom-made hood. The total air flow rate of the RTIs and samplers was approximately 2.205 L/min. The paper was printed with a total of 806 words in 10 point font per sheet with black toner only. The RTI measurements were collected for a 10 min background reading at the beginning of the experiment, an approximately 40–43 min reading during the printing portion of the experiment (including paper refilling and toner replacement time) and a 10 min post-experiment background reading. During the paper refilling and toner replacement, the printer was at rest with the motor stopped. These periods are marked as gray highlighted areas in Fig. 2a–2f and are denoted as ‘resting time’ in this study. The printing process was repeated three times, but the duration of resting time varied depending on the condition of the printer, such as the presence of a paper jam. All trials were performed under the same operating conditions with the same number of papers printed. The variations among repeated experiments were due to the resting time needed to clear paper jams and replace toners.

The measurements were taken approximately 0.14 m horizontally from the center of the printer exhaust port, and the average air velocity at this sampling location was approximately 0.3 m/sec. The entire surface of the hood was wiped with isopropyl alcohol before and after each experiment.

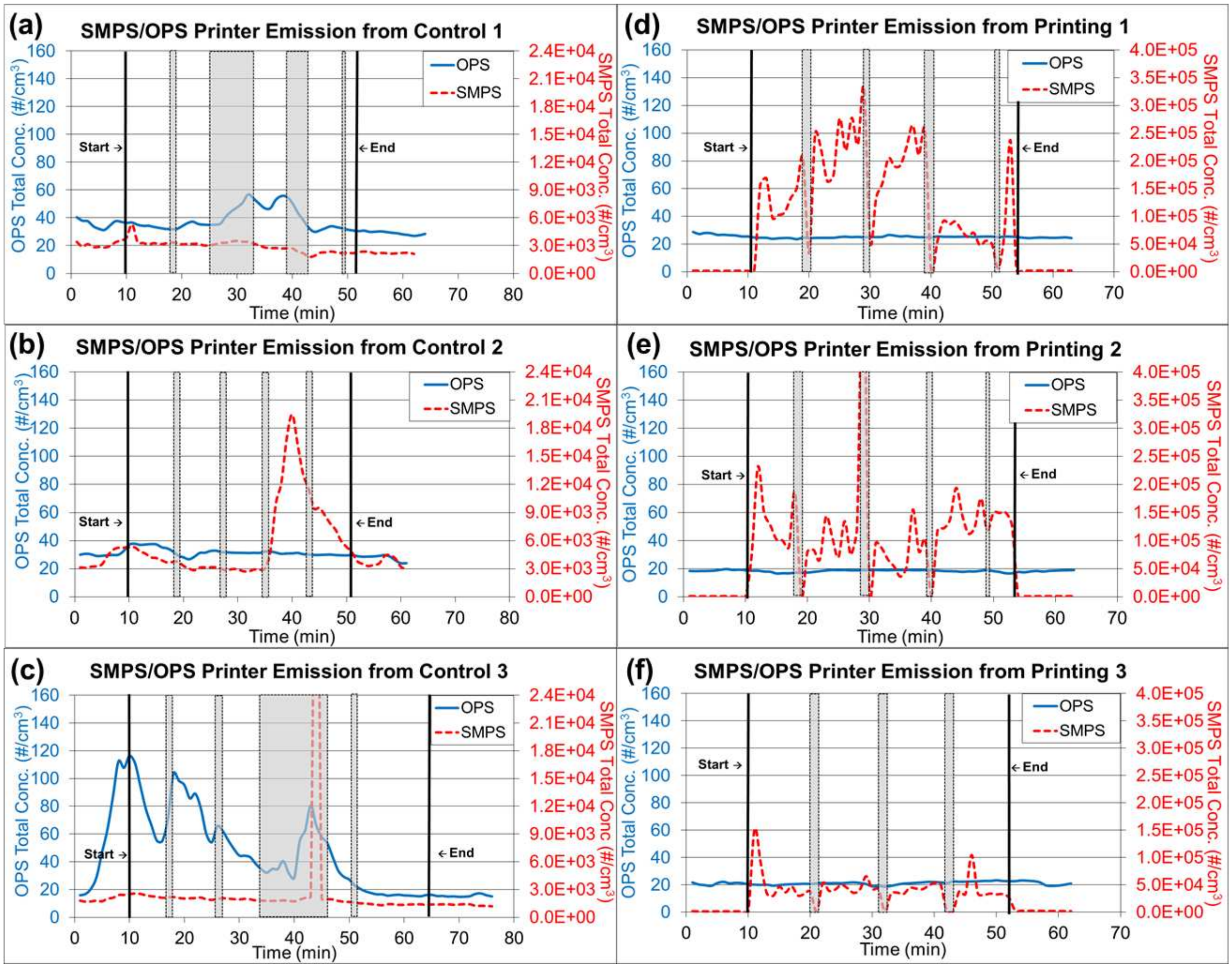

Figure 2. Real time instrument (RTI) data for emission tests from running 1,000 plain paper sheets and printing 1,000 sheets. (a)-(c) Total concentrations from three repeated experiments running 1,000 sheets each, as measured by RTIs. (d)-(f) Total concentrations from three repeated experiments printing 1,000 sheets each, as measured by RTIs.

*Note: Gray highlighted areas represent 'resting time' in Figure 2, which the printer was at rest with the motor stopped for paper refilling and toner replacement.

2.2) Paper Particles Emitted from Shredding Activities

Shredding was performed in a glove box (Series 100, Terra Universal, Fullerton, CA, USA) equipped with ultra-filtered clean air with the RTIs placed outside the glove box, as shown in Fig. 1b and 1c. The temperature inside the glove box was 20–22°C, and the relative humidity was between 8.6% and 15%. The average air velocity blown into the glove box at the filter inlet face, located on the ceiling of the glove box, was 2.7 m/s and the average outlet face velocity was 1.4 m/s. The air velocity range in which samplers were located was less than 0.05 m/s.

The shredder was placed on top of a box (0.25 m × 0.30 m × 0.20 m), and 0.9 m-long tubes were used to connect the RTIs to reach the sampling locations for measurements. Fig. 1b shows the top view of the experiment with the location of each device. Measurements were taken at approximately 15 cm above the center line of the shredder, as shown in Fig. 1c. Each device was located on each side of the box to avoid flow interruption, and the total air flow rate was the same as that in the printer particle release tests (2.205 L/min). The shredding experiments were performed with 40 sheets of 1) printed paper and 2) plain paper. The printed papers were obtained from the printer particle release test and shredded at 30-sec intervals for this evaluation. Each shredding experiment was repeated three times. The RTI data were exported into Excel and analyzed for particle number concentration and size distribution. The glove box was wiped clean with de-ionized water before and after each experiment, and the shredder was also wiped with isopropyl alcohol to remove any contamination before and after each experiment. All data were summarized to compare the released particle concentration and size during printing and shredding activities in the experiments.

2.3) Microscopy Analysis

After each experiment, the particles collected on TDS polycarbonate filters and copper grids were analyzed through electron microscopy. Small pieces of polycarbonate filters were coated with 10–15 nm gold and analyzed using scanning electron microscopy (SEM) (JSM-6500F, JOEL, Peabody, MA, USA) and energy dispersive spectroscopy (EDS) (model 51-XMX1015, Concord, MA, USA) at 15 kV. The grids were analyzed using TEM (JEM-2100F, JOEL, Peabody, MA, USA) and EDS (model 51-XMX1058, Concord, MA, USA) at 200 kV. These microscopy analyses were necessary for substances in micrometer to nanometer size range, to understand the morphological characteristics, sizes, and elemental compositions of the studied particles. The analyzed results will be able to identify typical particles and its constituents which might be exposure risks for humans..

2.4) In vitro Cytotoxicity Assays of Paper Particles Released by Shredding Activities

This analysis has been widely used as an indicator of potential biological toxic effects by measuring the viability of cells after exposure to studied particles.

2.4.1) Generation and collection of paper particles for cytotoxicity assays

The same shredding method as in the section *2.2) Paper particles emitted by shredding activities* was used with slight modifications to collect airborne paper particles for cytotoxicity evaluation. A total of 200 paper sheets, printed in black, with one sheet fed every 30 sec, were shredded into a 44 gallon bag placed underneath the shredder, and paper particles inside the bag were collected. The NIOSH manual of analytical methods (NMAM) 0500 method was used to collect particles in 37 mm cassettes with a polycarbonate filter instead of a PVC filter at a 1 L/min flow rate. The cassettes were located inside the bag. After shredding, the bag filled with shredded paper was shaken for 2 h for additional particle collection.

2.4.2) Preparation for Cytotoxicity Assays

The particles collected through the NIOSH NMAM 0500 method were weighed to obtain the mass, and the particles were then suspended in Dulbecco's modified Eagle's medium (DMEM) at a concentration of 10.77 mg/mL, which was the highest concentration (100%) exposed to cells in this experiment. The dose was determined to model the extreme scenarios for cell viability response on biomarkers caused by the exposure. The highest dose (100%) used was approximately 80,000 to 50,000 times higher than the average total mass concentration of paper particles collected using NIOSH NMAM 0500 method. Several dilutions (e.g., 100%, 50%, and 25%) of particle suspended media samples were prepared for variations on cell treatment. The prepared particle suspensions in media were further sonicated with a sonic dismembrator (model 100, Fisher Scientific, Hampton, NH, USA) for 20 min in an ice bath.

Cytotoxicity assays used the following human bronchial epithelial cell line models: simian virus-transformed bronchial epithelial cells (BEAS2B, CRL-9609, ATCC, Manassas, VA, USA) and immortalized normal human bronchial epithelial cells (HBE1, a kind gift from Dr. Reen Wu's laboratory, University of California, Davis, CA, USA) for treatments of 24–48 h. BEAS2B cells were isolated from normal human bronchial epithelium obtained from autopsies collected from individuals without cancer[19-24], and HBE1 cells were obtained from a 60-year-old female donor with idiopathic pulmonary fibrosis[25]. Thus, both cell lines are non-transformed.

BEAS2B cells were cultured in DMEM (11885-084, Thermo Fisher Scientific, Waltham, MA, USA) with 10% fetal bovine serum and 1% penicillin/streptomycin (97062-806, VWR, Radnor, PA, USA). HBE1 cells were cultured in DMEM/F12 (D6434, Sigma-Aldrich, St. Louis, MO, USA) with supplements including 2.5 mM L-glutamine (G7513, Sigma-Aldrich), 2.5 μg/mL plasmocin (ant-mpt, InvivoGen, San Diego, CA, USA), 1.5 mg/ml bovine hypothalamus extract (C-30180, BioMedica, PromoCell, USA), 4 μg/ml insulin (#I6643, Sigma-Aldrich), 5 μg/ml transferrin (#T8158, Sigma-Aldrich, St. Louis, MO, USA), 10 ng/mL EGF (#E9644, Sigma-Aldrich), 0.1 μM dexamethasone (D4902, Sigma-Aldrich) and 20 ng/ml cholera toxin (C8052, Sigma-Aldrich). Both cell lines were incubated in a humidified incubator at 37 °C with 5% CO_2.

2.4.3) In vitro Cytotoxicity Assays

HBE1 and BEAS2B cells were grown to confluence in 96 well plates (15705-066, VWR, Radnor, PA, USA) before paper particle exposure. Serum deprivation was then initiated 24 h before paper particle treatment for the BEAS2B cells and was followed by treatment with two types of paper particles (plain and printed) for 24–48 h. CellTiter 96 AQueous One Solution Cell Viability assays (MTS assay, Promega, Madison, WI, USA) were then performed to detect cytotoxicity according to the manufacturer's protocol. HBE1 cells were treated with the particles in their medium which is serum-free, similarly to the cells in BEAS2B medium, and cytotoxicity was tested 24–48 h after treatment.

Plates were read at 490 nm with a microplate reader (Infinite 200 PRO NanoQuant Microplate Reader, Tecan, Morrisville, NC, USA). Each concentration was assessed in three replicates per experiment, and the experiments were repeated three times. The cell viability results of three replicates were calculated to determine the standard error of the mean and were standardized by calculating the percentage change relative to control (set at 100%) for each plate.

2.4.4) Statistical Analysis

Statistical analysis was conducted with the SPSS statistical analysis software package (version 1.0.0.1126, IBM, Armonk, NY, USA). The cell viabilities of two cell lines (BEAS2B and HBE1) treated with various concentrations of paper particles were assessed and evaluated for statistical significance with one-way analysis of variance. At a 95% confidence level, p-values < 0.05 were considered statistically significant.

2.5) SP-ICP-MS Analysis

A portion of particle-containing media prepared for cell exposure was analyzed for elemental composition using single particle inductive coupled plasma-mass spectrometry (SP-ICP-MS) with a NexION 350D mass spectrometer (PerkinElmer, Bradford, CT, USA) connected to a self-aspirating nebulizer (PFA-ST nebulizer) (Elemental scientific, Omaha, NE, USA) and a Peltier (PC3x, Elemental Scientific, Omaha, NE, USA) controlled quartz cyclonic spray chamber (Elemental Scientific, Omaha, NE, USA) set at 2 °C. Samples were centrifuged to remove agglomerates and were diluted 100 times with 2% HNO_3. Samples were introduced with autodilution equipment (prepFAST SC-2 autosampler) (Elemental Scientific, Omaha, NE, USA). Before analysis, the nebulizer gas flow and quadrupole ion deflector were optimized for maximum indium signal intensity. A daily performance check was also performed to ensure that the instrument was operating properly and that a CeO^+ to Ce ratio less than 0.025 and a Ce^{++} to Ce ratio less than 0.030 were obtained. After suspending the particles in the media, the liquid suspension was injected into the SP-ICP-MS; the detection showed the sizes and elements of nanoparticles. This test was repeated three times. The differences in elemental composition were compared to the blank medium and analyzed with Syngistix's software (PerkinElmer, Bradford, CT, USA).

CHAPTER 3

RESULTS AND DISCUSSION

3.1) Printer Emission Tests

The measured particle concentrations obtained from RTIs were analyzed and are presented in two types of graphs showing 1) the total particle number concentration changes throughout the entire experiment and 2) the size-fractionated particle number concentration.

The total concentration of each experiment is presented separately in Fig. 2a–2c for running 1,000 sheets (control) and in Fig. 2d–2g for printing 1,000 sheets due to the inconsistent resting periods. The experimental periods (pre-experiment, during printing, during resting time and post-experiment) were noted. The average total concentrations and standard deviations throughout the experimental periods were calculated and presented in Table 1.

Table 1. Average total concentrations from printer particle release tests, as measured by NanoScan SMPS and OPS.

Average Total Concentration and Standard Deviation of Printer Particle Release Tests (particles/cm^3)				
	OPS		SMPS	
	Plain (control)	Printing	Plain (control)	Printing
Pre-experiment	43 (±14)	22 (±0.41)	3,100 (±510)	1,400 (±60)
During printing	41 (±10)	22 (±0.61)	3,600 (±1,500)	100,000 (±24,000)
Resting time	44 (±17)	21 (±3)	4200 (±8,200)	110,000 (±160,000)
Post-experiment	24 (±1)	21 (±0.41)	2,400 (±184)	1,800 (±153)

Note: Standard deviations are presented in parentheses.

During printing, the concentration difference between running and printing 1,000 sheets, as determined by NanoScan SMPS, was 98,100 particles/cm^3.

Concentration changes during printing were calculated in this section by subtracting the pre-experiment concentration, and the background concentration, to adjust the particle concentrations from the environment in the laboratory room. During the printing periods for printing 1,000 sheets, the total net concentration of particles smaller than 420 nm (NanoScan SMPS data) increased by approximately 98,600 particles/cm^3 from 1,400 particles/cm^3 to 100,000 particles/cm^3. However, the net increase of running 1,000 sheets was approximately 500 particles/cm^3 from 3,100 particles/cm^3 to 3,600 particles/cm^3, thus indicating a 200-fold difference between printing and running 1,000 sheets. The laboratory where this experiment was performed has the average background concentration of 7,000 particles/cm^3 for particle size less than 420 nm and 7 particles/cm^3 for particle size range from 0.3 to 10 μm. The particles released during printing 1,000 sheets had 14 and 7 times higher average concentrations than the laboratory background, in particle sizes less than 420 nm and in a range of 3-10 μm respectively. Printing 1,000 sheets resulted in a substantial increase in concentration, as also seen through the comparison to the resting time values indicated in gray highlights in Fig. 2d–2g. This increase caused by printing paper was apparent on sub-micrometer sized particles measured by NanoScan SMPS but not on larger particles measured by OPS. Currently, there are no health guidelines or standards for particulate number concentrations in the U.S. However, the contribution of high number particle concentration by printing processes to the indoor environments may become a concern.

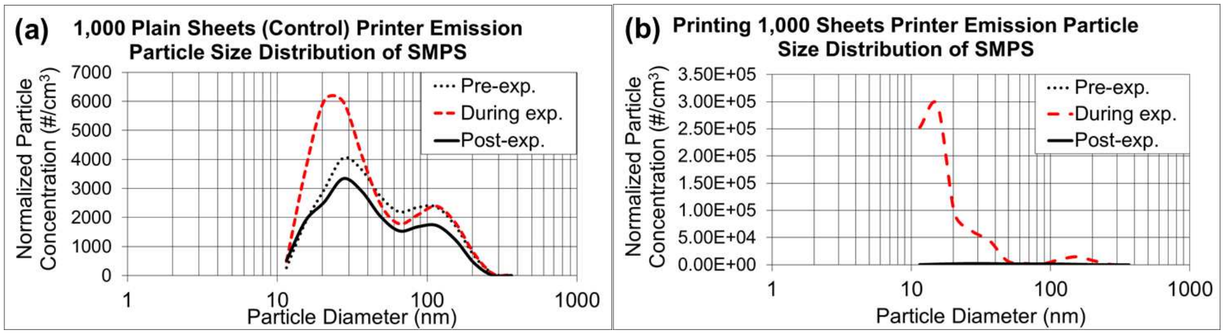

Figure 3. NanoScan SMPS data of emitted particle size distribution. (a) Average particle size distributions of three repeated experiments running 1,000 sheets each, as represented in Fig. 2a–2c. (b) Average particle size distributions of three repeated experiments printing 1,000 sheets each, as represented in Fig. 2d–2f.

In the control experiments presented in Fig. 3a and 3b, the dominant particle size generated from running 1,000 sheets peaked at 27 nm, as determined through NanoScan SMPS, and the average concentration was approximately 6,000 particles/cm^3 during the experiment. Although this corresponding mode size had a relatively higher concentration than the pre- and post-experiment concentrations, the mode sizes remained same at 27 nm throughout the entire experiment. As discussed previously, when the toner was used for printing of 1,000 sheets, the mode size appeared to be smaller (15 nm), with a concentration of approximately 300,000 particles/cm^3. Thus, the printing process generated substantially more particles with smaller sizes within 10–420 nm than were generated by running the printer. The amount of released particles with larger than sub-micrometer diameters, as measured by OPS (0.3–10 µm), did not differ between printing and the control process of running the printer, as presented in Fig. 4a and 4b. The OPS mode sizes were 337 nm for both experiments, with a concentration range of 150–350 particles/cm^3.

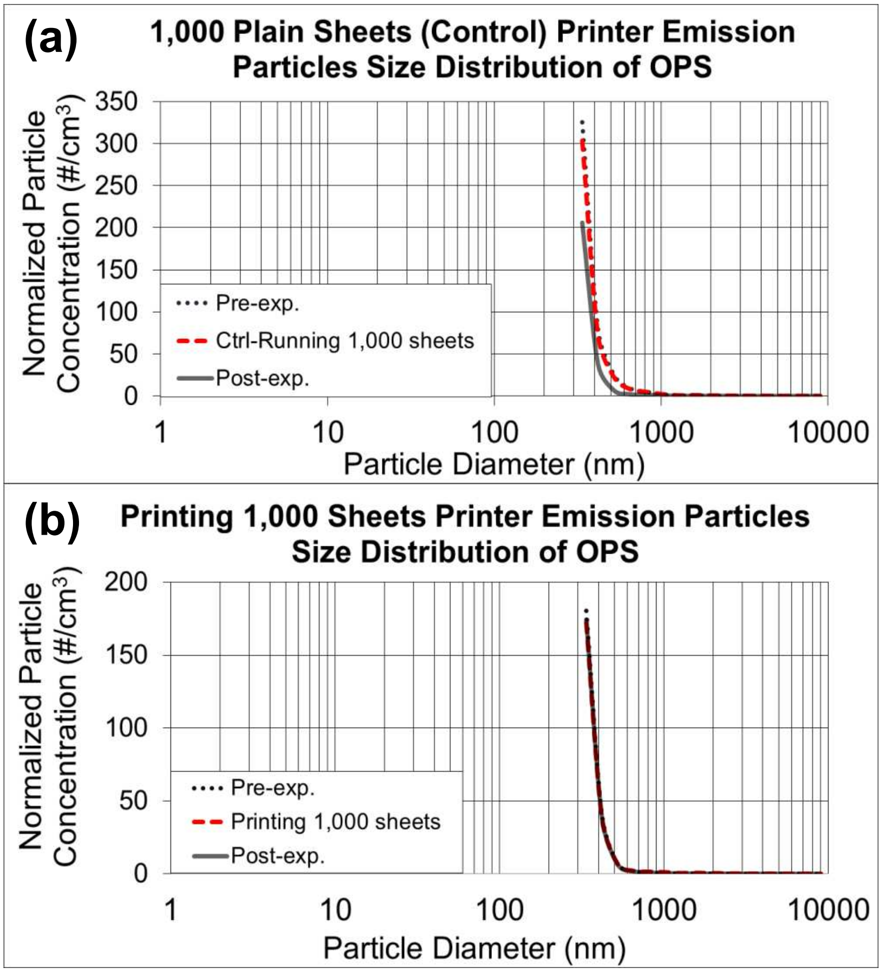

Figure 4. Real time instrument (RTI) data of emission tests from running 1,000 plain paper sheets and printing 1,000 sheets. (a) Particle size distribution for running 1,000 plain sheets, as determined by OPS (0.3–10 μm). (b) Particle size distribution for printing 1,000 sheets, as determined by OPS.

3.2) Morphology and Elemental Composition Analysis of Printer Emissions

The printer released particles collected through TDS were in various shapes and sizes. The typical shapes of the particles were granular, irregular and layered. These particles were consistently found through microscopy analysis of samples collected during printing (Fig. 5a–5d, 6a–6f, 7a and 8a). The sizes of the particles observed under TEM and SEM were in the sub-micrometer range, which corresponded to the RTI measurements of 1 μm or less.

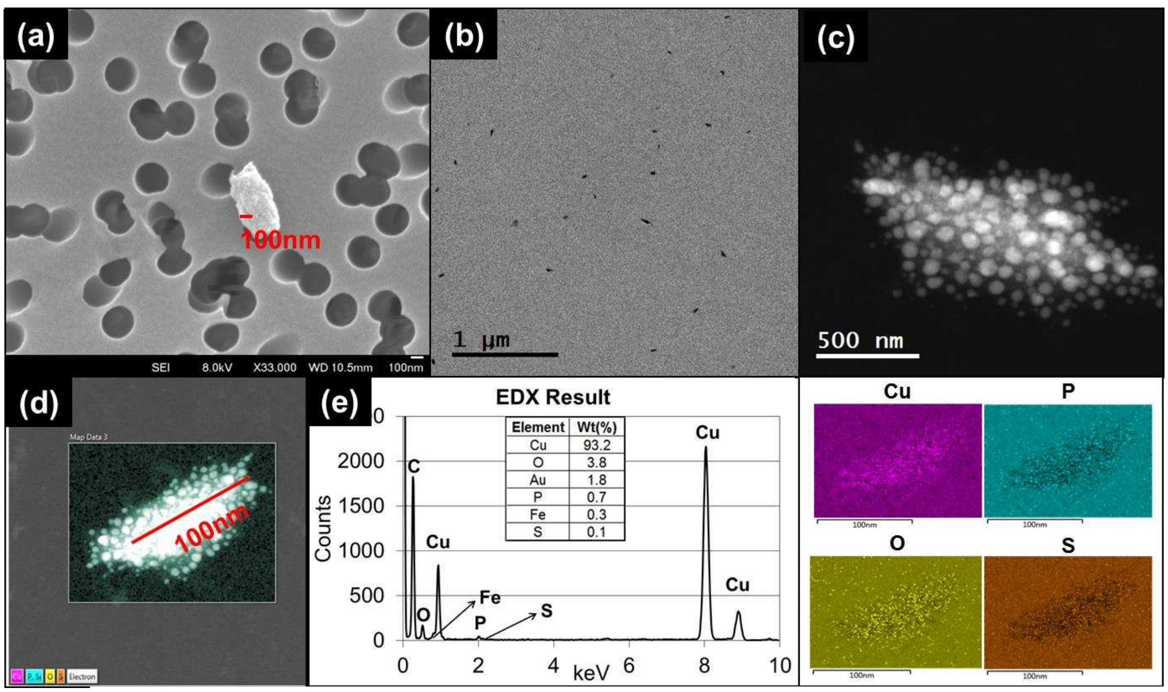

Figure 5. Microscopy analysis (SEM/TEM/EDS) of printer emitted particles. (a) SEM image of printer emitted particles on a TDS polycarbonate filter. (b) TEM image showing collected printer emitted particles on a TDS copper grid at low magnification. (c) TDS TEM image of printer emitted particles, with many attached granular particles, at high magnification. (d) TEM-EDS image of analyzed particles with attached granules, as observed through TDS. (e) EDS quantitative analysis of the image in (d) and qualitative analysis indicated by color.

Note: Gold (Au) was used as a coating, which was excluded in this analysis.

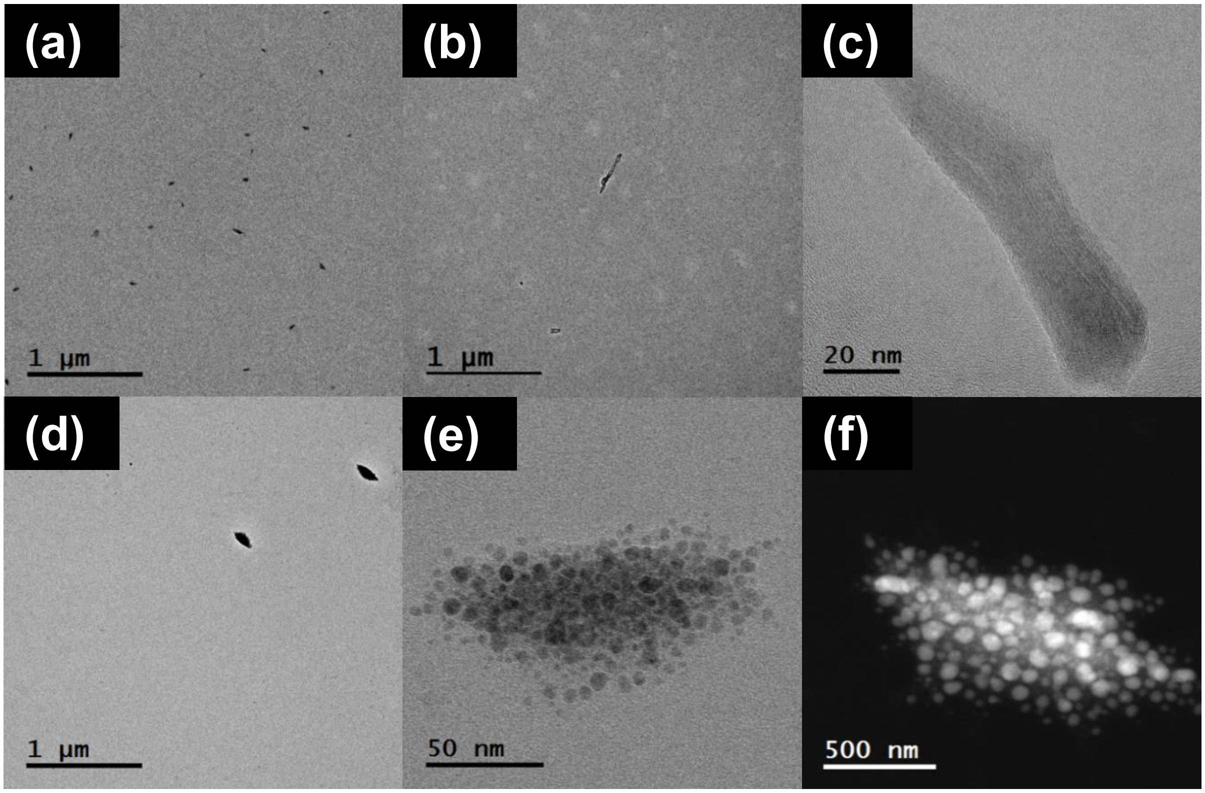

Figure 6. Microscopic analysis (TEM) of printer emitted particles collected on a TDS Cu grid. Various shapes of particles were observed.

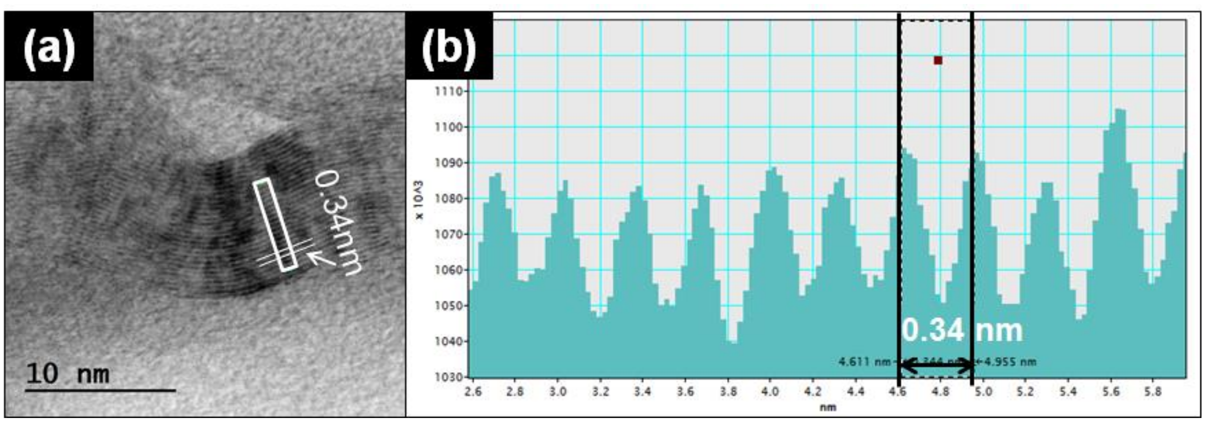

Figure 7. Graphite TEM lattice analysis. (a) Representative TEM image of graphite particles emitted from the printer (b) The intensity line profile of the selected area from (a).

Fig. 5a–5d shows the results of granular and irregular shaped particles in TEM analysis and Fig. 5e shows the elemental composition of the particles in EDS analysis. For these particular particles, each granule ranged in size between 1 and 10 nm, and the major elemental composition comprised C, Cu, P, and S. Regardless of whether copper grids were used, Cu was found to account for a major portion of the particle composition. The blank copper grid in EDS analysis showed a 1:5 ratio between the Lα-shell and Kα-shell, whereas the copper-containing granular particles displayed a stronger peak ratio between the Lα-shell and Kα-shell (1:3 ratio or higher; Fig. 5e), compared with the other types of particles (Fig. 8).

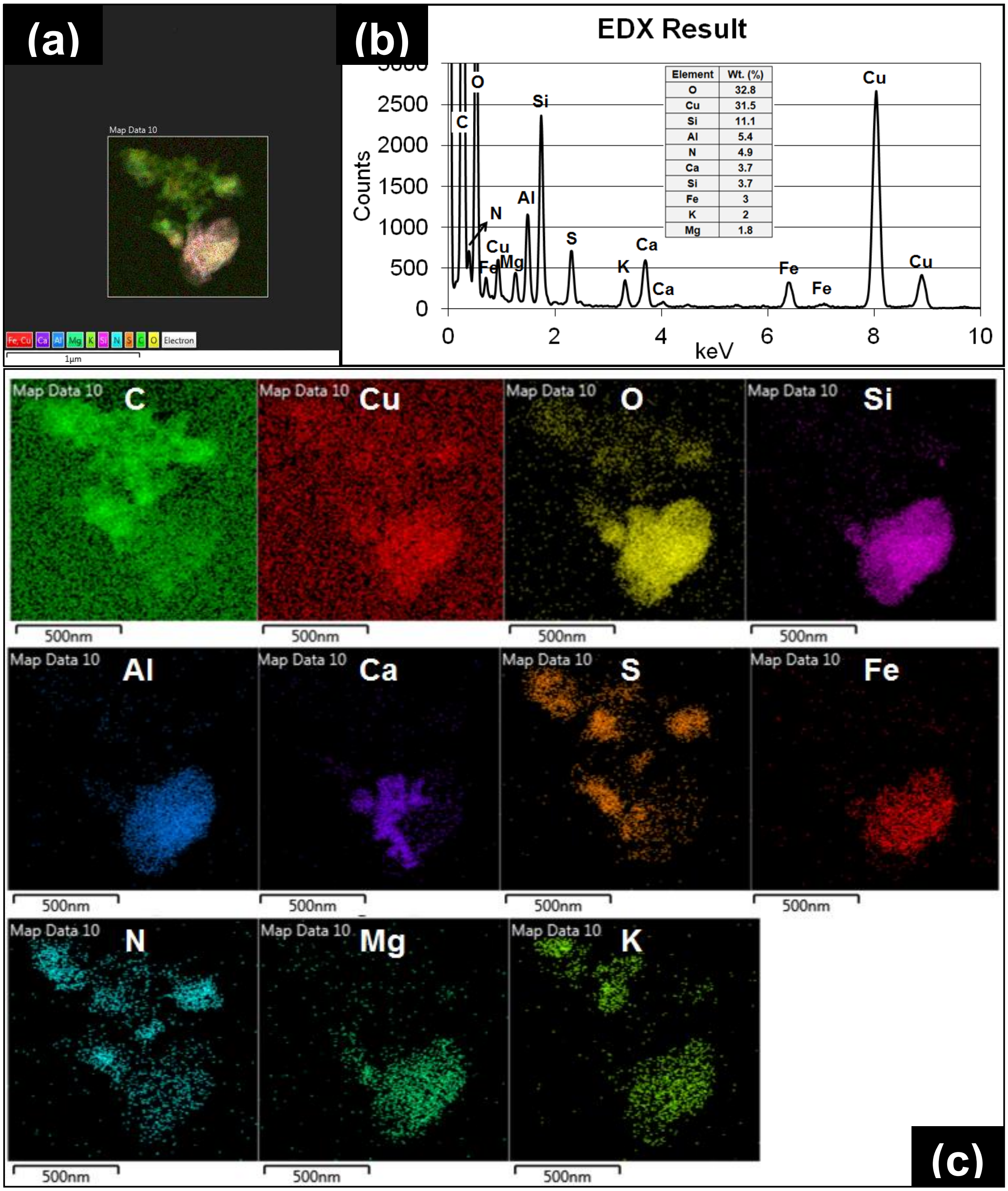

Figure 8. Printer emission particle analysis via EDS, showing granules attached in one particle, as determined using TDS.

Another typical observed particle was irregular and layered (Fig. 6c and 7a). To identify the characteristics of this type of particle, we used TEM line profile analysis to measure the distance between layers. The interlayer space measurement of the particle was 0.34 nm, a typical carbon bond length. This structural property is commonly identified as graphite, a multi-layer form of carbon, through the established analysis method[26].

Other than the granular and layered particles, the irregular shaped particles observed under TEM were also analyzed with EDS. The EDS results showed various types of metals from the particles released from both running and printing 1,000 sheets. Fig. 8a shows irregular shape particles collected by using TDS and analysis through EDS. The peaks in Fig 8b show various elements and intensities for each element, including Al, Ca, C, Cu, Fe, K, Mg, N, O, S and Si. The distribution map of each element in the particle is presented in Fig. 8c.

On the basis of our findings, multiple factors can contribute to the constituents of released particles from printing, such as metal-containing parts inside the printer and the heat generated during printing. The high level of nanoparticle release from a printer can cause respiratory problems and indoor air quality issues in similar environments, such as commercial printing rooms or any locations where printers are in use. As also stated in the NIOSH Pocket Guide to Chemical Hazards, copper may be associated with adverse health effects, such as acceleration of mutation in respiratory tract, skin, liver and kidney cells. Different printers may emit particles with different characteristics and airborne concentrations.

3.3) Paper Particles Emitted From Shredding Activities

The particle concentrations measured from shredding activities were compared among the pre-experimental background, the shredding process and the post-experimental background, and the changes in particle concentration and size distribution were observed (Fig.9a–9c). As presented in Fig. 9a, the paper particle concentration in the 10–420 nm size range (NanoScan SMPS) increased at the beginning of the shredding, and the concentration in the 0.3–10 μm size range (OPS) increased at the end of the shredding experiment. Table 2 summarizes the average concentrations of various particle sizes on both instruments by the first- and second-half (10 min) of shredding time (20 min). There was no indication of a mode size change between the first- and second-half of shredding for OPS measurements. The mode size on OPS was determined to be the same as 337 nm on both the first- and second-half of the shredding period, and as expected the overall concentrations of all sizes on second-half of shredding period were higher than the first half. The mode size of NanoScan SMPS measurements varied from 20.5 to 36.5 nm and the concentrations did not give a clear indication of concentration increase as seen on OPS measurements. The released paper particles had similar average concentrations of 77–82 particles/cm^3, on the basis of OPS measurements, regardless of whether plain (control) or printed paper was shredded. However, Table 3, the findings regarding released particles less than 420 nm (NanoScan SMPS) showed that shredding printed paper released three times fewer particles than shredding plain paper. This result was notable in terms of the size distributions and upper standard deviations (Fig. 9b and 9c). The mode size of the released printed paper particles was 27 nm with a concentration of 10,000 particles/cm^3, whereas plain paper had a mode size of 37 nm with a concentration of 26,000 particles/cm^3, a value 2.6 times greater. The high variations of standard deviations (Fig. 9b) are due to the loosely structured plain paper that was not pressed with the toner through the heating process. More small particles were released from plain paper than printed paper due to the structural alteration, as confirmed by the TEM and SEM analyses.

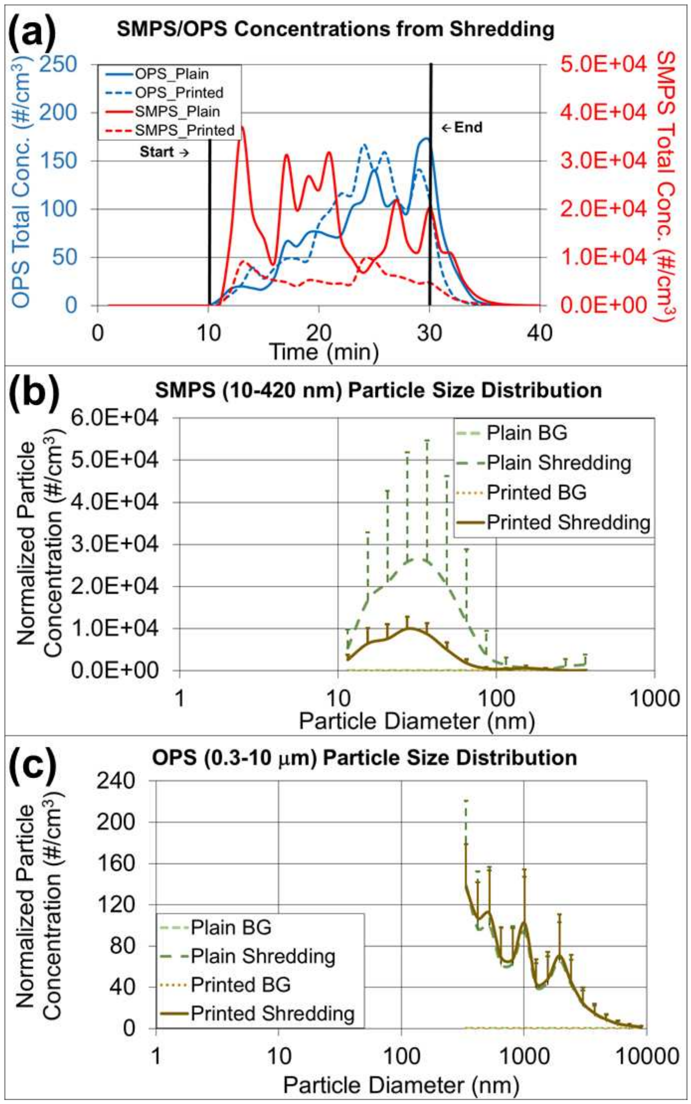

Figure 9. RTI [OPS (0.3–10 μm) and SMPS (10–420 nm)] data for shredding 40 sheets of plain and printed paper. (a) Area total particle concentration, as measured by RTIs. (b) Paper particle size distribution, as determined by NanoScan SMPS. (c) Paper particle size distribution, as determined by OPS.

Table 2. Average particle concentrations of one-half fractions of each experiment during shredding only by particle size

Average particle number concentration (# particles/ experiment period) on OPS																	
Particle size (nm)		**337**	**419**	**522**	**650**	**809**	**1,007**	**1,254**	**1,562**	**1,944**	**2,421**	**3,014**	**3,752**	**4,672**	**5,816**	**7,242**	**9,016**
Plain 1	1st half	**49**	35	37	24	24	36	16	17	26	17	10	6	3	2	1	1
	2nd half	**222**	182	199	126	128	192	83	91	135	86	48	28	16	9	5	3
Plain 2	1st half	**127**	59	49	29	28	40	17	19	27	17	10	6	3	2	1	1
	2nd half	**211**	144	145	90	90	131	56	62	89	58	32	19	12	6	4	2
Plain 3	1st half	**71**	46	45	28	28	43	18	21	31	20	11	7	4	2	1	1
	2nd half	**114**	89	96	62	64	95	42	47	69	45	26	15	9	5	3	2
Printed 1	1st half	**49**	34	33	20	19	27	12	13	19	13	7	4	3	1	1	1
	2nd half	**202**	158	159	94	89	127	53	58	82	51	28	17	10	5	3	2
Printed 2	1st half	**58**	43	43	26	25	36	15	17	25	16	9	5	3	2	1	1
	2nd half	**143**	115	117	70	67	99	41	45	64	40	21	12	7	4	2	1
Printed 3	1st half	**96**	69	73	47	45	72	31	34	52	33	19	11	7	4	2	1
	2nd half	**270**	223	245	157	158	252	110	122	182	118	65	39	23	12	7	4

Average particle number concentration (# particles/ experiment period) on SMPS														
Particle size (nm)		**11.5**	**15.4**	**20.5**	**27.4**	**36.5**	**48.7**	**64.9**	**86.6**	**115.5**	**154**	**205.4**	**273.8**	**365.2**
Plain 1	1st half	2,814	5,166	5,305	**7,567**	6,950	4,120	1,237	213	214	222	150	86	37
	2nd half	2,739	7,193	8,517	**10,861**	9,309	5,336	1,910	532	589	779	440	111	147
Plain 2	1st half	12,750	51,678	70,223	77,163	**79,935**	69,292	44,462	12,641	4,949	2,112	32	5,490	8,089
	2nd half	9,568	23,285	27,860	41,677	**45,634**	37,146	21,989	8,989	2,520	745	705	1,185	1,253
Plain 3	1st half	3,609	8,564	11,139	**15,061**	13,100	7,443	2,238	418	332	371	151	55	27
	2nd half	2,197	8,236	8,894	**10,314**	8,411	4,597	1,183	132	245	379	280	129	79
Printed 1	1st half	2,274	5,144	5,640	**7,166**	6,409	3,959	1,463	354	302	194	72	165	135
	2nd half	3,751	5,600	6,899	14,419	**14,721**	8,717	3,649	1,302	762	1,643	1,127	27	125
Printed 2	1st half	1,538	3,509	4,679	**6,921**	5,932	3,011	602	95	284	509	289	42	37
	2nd half	1,024	3,498	5,243	**6,876**	5,846	3,309	1,058	305	256	316	197	28	20
Printed 3	1st half	3,938	9,902	10,827	**12,638**	11,212	7,315	3,262	852	351	325	87	132	218
	2nd half	3,248	11,295	**12,340**	12,110	8,446	3,815	851	363	716	855	446	43	5

Table 3. Average total concentration from shredding experiments, as measured by NanoScan SMPS and OPS.

Average Total Concentration and Standard Deviation of shredding by Time Period (particles/cm^3)				
	OPS		NanoScan SMPS	
	Plain (control)	Printed	Plain (control)	Printed
Pre-experiment	0.011 (±0.0062)	0.034 (±0.089)	5.4 (±3.1)	1.3 (±0.75)
During shredding	77 (±49)	82 (±51)	17,000 (±9,400)	5,600 (±2,200)
Post-experiment	17 (±29)	6.1 (±13)	3,200 (±4,500)	710 (±1,000)

Note: Standard deviations are presented in parentheses.

3.4) Analysis of Paper Surface and Elemental Composition

To determine the structures of printed paper and plain paper, the surfaces of paper pieces and elemental composition analysis were conducted by using TEM (Fig. 10a–10e), SEM and EDS (Fig. 11a and 11c). The surface of the plain paper (Fig. 11a) showed entangled fibers with nano- to micro-meter sized particle agglomerates. The surface of the printed paper (Fig. 11c) had a melted appearance similar to basalt, possibly as a result of the heat pressing during printing with the toner. The composition analysis showed that the printed paper contained Al, Ca, Cl, S and Si (Fig 11d) and Na, Mg, and P elements were found from both the printed paper and plain paper (Fig. 11b).

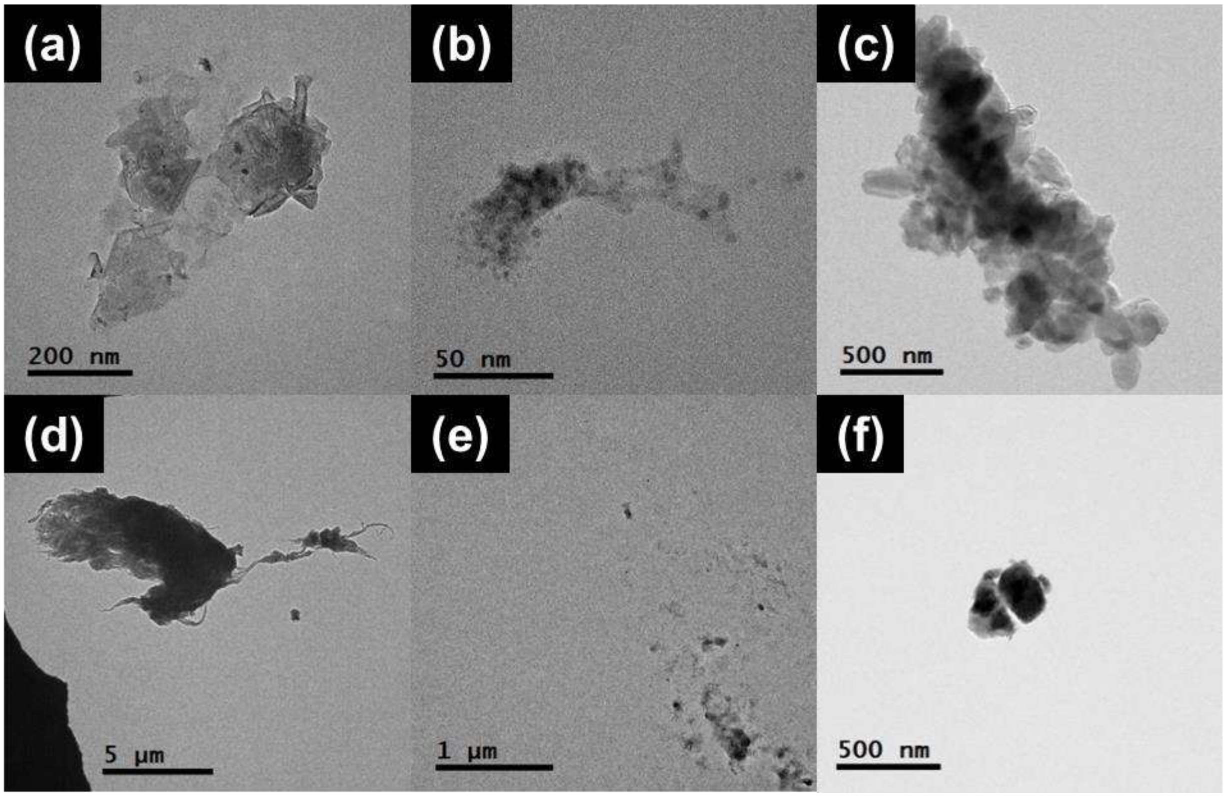

Figure 10. Paper particles observed from the shredding process. Various shapes of particles were observed through TEM.

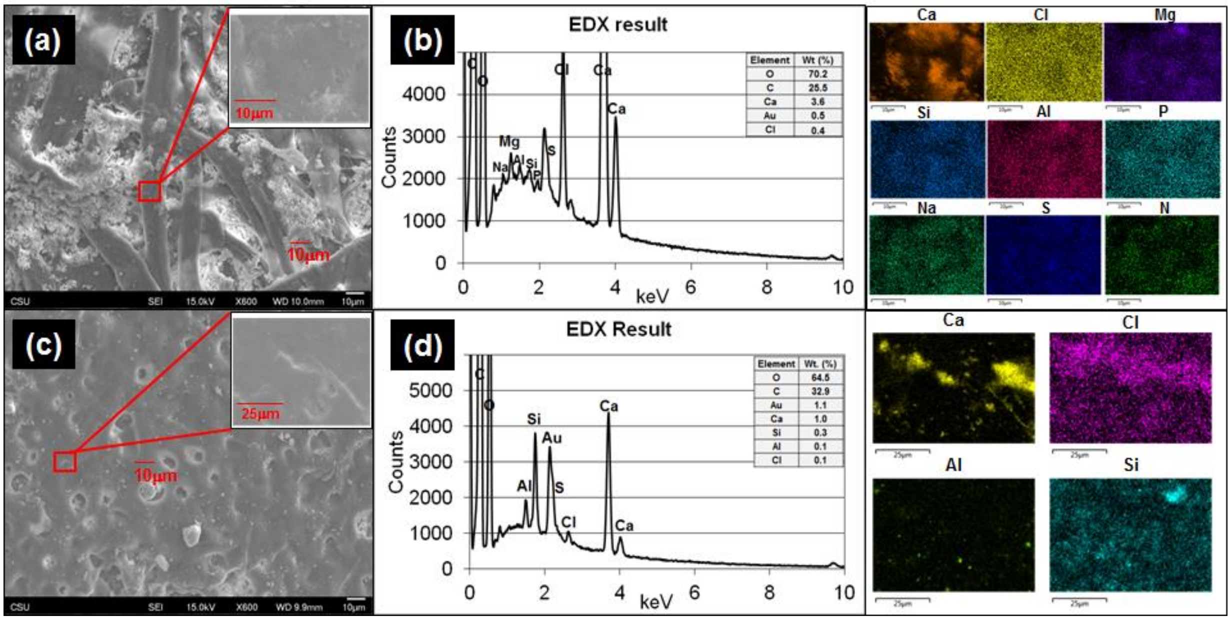

Figure 11. Microscopy analysis of paper particles from shredding plain and printed paper. (a) SEM images of plain paper at low and high magnification. (b) EDS quantitative and qualitative analyses of image (a), plain paper. (c) SEM images of printed paper at low and high magnification. (d) EDS quantitative and quantitative analysis of image (c), printed paper.

3.5) Cytotoxicity Effects of Released Paper Particles and Elemental Composition Analysis

In the cytotoxicity study, two human lung cell lines (BEAS2B and HBE1) were treated with paper particles, and the cytotoxicity responses of the cells to the particles were measured (Fig. 12a and 12b). The cytotoxicity varied substantially and yielded inconsistent results according to statistical analysis (p-value > 0.05, determined at 95% confidence level, for exposed concentration levels in all types of experiments). For the treated BEAS2B cells, the cytotoxicity results after exposure to various concentrations did not show significance among different concentrations of paper dust treatment for both plain paper particles (p-value of 0.866) and printed paper particles (p-value of 0.603). Similarly, for the treated HBE1 cells, the cytotoxicity responses after exposure to plain paper particles (p-value of 0.324) and printed paper particles (p-value of 0.732) at various concentrations did not show significance. In summary, treatment with all concentrations in both cell lines did not yield significant changes in cell viability and appear to increase cell number; thus, there is no evidence that the various levels of paper particle concentrations to which the BEAS2B and HBE1 cells were exposed had significant toxicity effects in terms of cellular response.

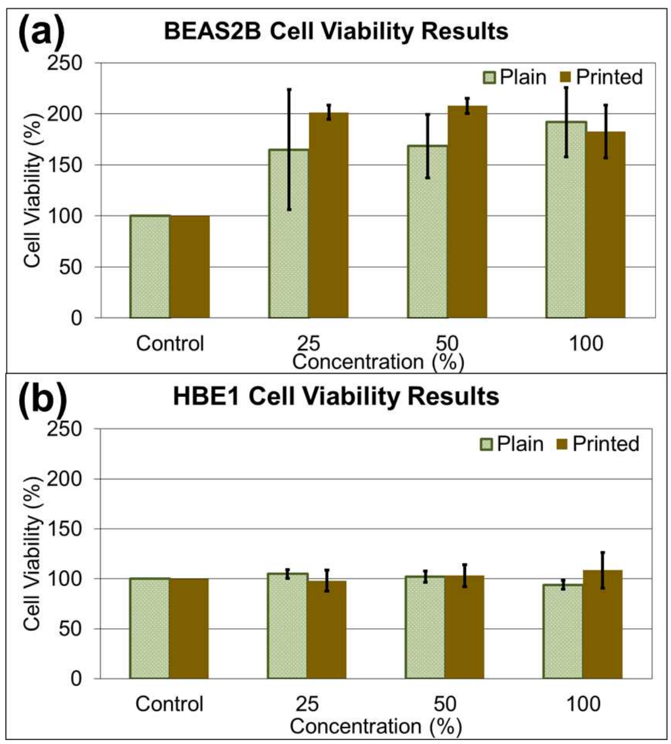

Figure 12. Cell viabilities in two different cell lines (BEAS2B and HBE1) after paper particle exposure for 24-48 h. The mean values of each concentration are presented in bar graphs as a percentage with respect to the control in each cell line not exposed to paper particles. Error bars are standard error of the mean. (a) Changes in viability in the BEAS2B cell line. (b) Changes in viability in the HBE1 cell line.

Investigating the effect of paper particle exposure on human lung cells is important because of the exposure possibilities to humans in various indoor environments. Although the cytotoxicity results of paper particle exposure showed inconsistency across various concentrations, and no significant differences were observed, this result may not represent the response from human exposure. The cytotoxicity response in humans may differ depending on the particle size, an individual's physical and medical status and susceptibility to the constituents in the paper particles. For example, individuals with asthma may be more susceptible to these particles due to potential co-exposure effects [27, 28], the focus of future studies. In addition, many toxicants are not cytotoxic yet still exert biological effects in the human body; for example, some polycyclic aromatic hydrocarbons can lead to inflammatory mediator production at non-toxic doses in lung epithelial cells[29]. Regardless of the uncertainty of cytotoxicity, the nanometer-sized particles released by the shredding process are still of concern because of their deposition in the alveolar region after inhalation and their potential to enter the bloodstream.

Additionally, the medium alone and the particle suspended medium used for cell treatment were analyzed with SP-ICP-MS to identify the potential elements affecting cytotoxicity. Fig. 13a and 13b show the average intensity of each element (as the average relative intensity difference relative to blank media from three replicates with standard errors). The original SP-ICP-MS measurement report is presented in Appendix: A Table A1. The elements Br, Ca, Fe and P were identified from both plain and printed paper, and Al, Cu, and Ni were additionally found from only plain paper. A comparison of SP-ICP-MS and EDS analysis indicated that the elements Al, Ca, and P were commonly identified from plain paper, and Ca from printed paper, on both instruments. However, the remaining elements identified from SP-ICP-MS, such as Br, Cu, Fe, and Ni from plain paper, and Br, Fe, and P from printed paper, did not overlap with the EDS results. Cl, Mg, Na, S, and Si, the other elements identified in EDS analysis, were not detected in SP-ICP-MS analysis. The elemental composition analysis of paper particles showed limited overlapping constituents in SP-ICP-MS and EDS analysis. This discrepancy may be explained by the sample preparation process for SP-ICP-MS analysis, such as centrifuging, dilution, and removal of some paper particles to form evenly suspended solution, the variation of instrument detection limits and operating sensitivity. The EDS analyzes samples directly on particle or paper without processing any treatment or further laboratory procedures. As observed from the results, the use of different analytical instrument may alter the composition of samples due to the sample preparation procedures.

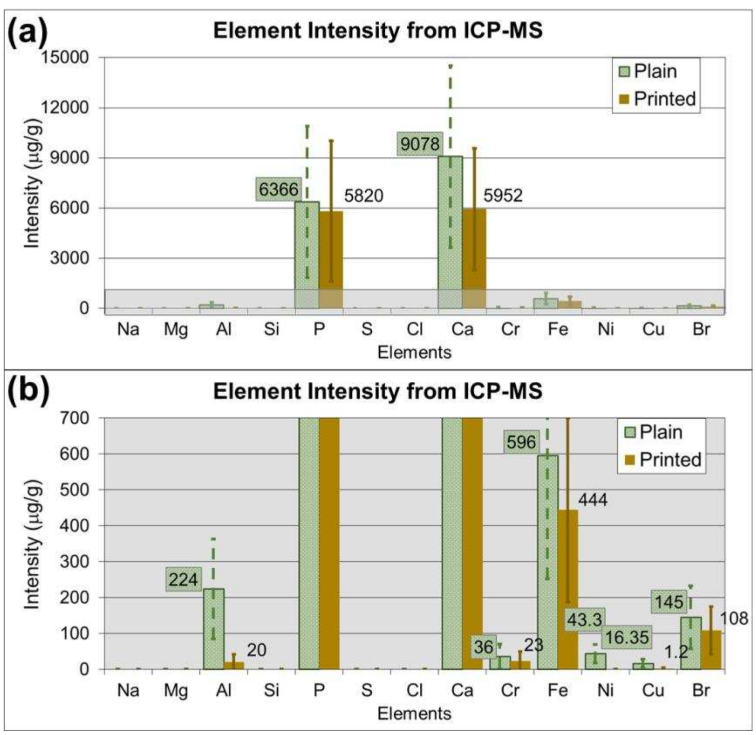

Figure 13. Average element intensities of paper particles in media used for cytotoxicity assays, with standard error bars of each mean measured by SP-ICP-MS, representing the net intensity difference after subtraction of the blank sample. (a) Overall intensity results in a scale up to 15,000 µg/g. (b) Intensity results in a scale less than 700 µg/g of the highlighted area in (a).

CHAPTER 4

CONCLUSIONS

In conclusion, this study showed substantial particle release from printer printing and that those particles contained various elements. Shredding of printed paper released fewer particles than shredding of plain paper. A review article regarding indoor air qualities of PM 2.5 and PM 10 has reported the particle concentrations measured at various locations (homes, schools, offices and aged care facilities). Comparisons of the measurements using different instruments are challenging because some instruments measure particle in aerodynamic size or mobility size. Our measurements using NanoScan SMPS and OPS have shown the particle number concentrations in a range of hundreds to thousands of particles per cubic centimeters for particles less than 2.5 μm, which represent PM 2.5. Other studies have shown the PM 2.5 measurements in the range from 1,200 to 1.2 x 10^6 particles/cm^3 at various indoor locations[30]. The contribution of particles released from printer and shredder use to the indoor air in such environments will add to the indoor particles and may become of concern, especially for susceptible people. The cytotoxicity tests on BEAS2B and HBE1 cells exposed to paper particles showed no toxicity; thus, the findings are inconclusive regarding additional potential health effects. However, the metal elements found on paper pieces and particles are known to have adverse health effects after excessive exposure; the health outcomes from such exposure may vary depending on an individual's susceptibility and health condition. Additional cellular endpoints, such as inflammatory mediators and wound healing, will need to be further evaluated in the future.

REFERENCES

1. A. J. Koivisto, T. Hussein, R. Niemelä, T. Tuomi and K. Hämeri, Impact of particle emissions of new laser printers on modeled office room, *Atmospheric Environment*, 2010, **44**, 2140-2146.
2. J. Sundell, H. Levin, W. W. Nazaroff, W. S. Cain, W. J. Fisk, D. T. Grimsrud, F. Gyntelberg, Y. Li, A. K. Persily, A. C. Pickering, J. M. Samet, J. D. Spengler, S. T. Taylor and C. J. Weschler, Ventilation rates and health: multidisciplinary review of the scientific literature, *Indoor Air*, 2011, **21**, 191-204.
3. C. Paolo and W. Peder, Assessment of Indoor Air Quality Problems in Office-Like Environments: Role of Occupational Health Services, *International Journal of Environmental Research and Public Health*, 2018, **15**, 741.
4. E. R. Jayaratne, X. Ling, C. He and L. Morawska, Monitoring charged particle and ion emissions from a laser printer, *Journal of Electrostatics*, 2012, **70**, 333-338.
5. S. Melching-Kollmuss, W. Dekant and F. Kalberlah, Investigations on fine and ultrafine particles released from laser printers and photocopiers as indoor air contaminants in German office rooms, *Naunyn-Schmiedebergs Archives Of Pharmacology*, 2009, **379**, 90-91.
6. S. Karrasch, M. Simon, B. Herbig, J. Langner, S. Seeger, A. Kronseder, S. Peters, G. Dietrich-Gumperlein, R. Schierl, D. Nowak and R. A. Jorres, Health effects of laser printer emissions: a controlled exposure study, *Indoor Air*, 2017, **27**, 753-765.
7. C. He, L. Morawska and L. Taplin, Particle Emission Characteristics of Office Printers, *Environmental Science & Technology*, 2007, **41**, 6039.

8. J. H. Byeon and J.-W. Kim, Particle emission from laser printers with different printing speeds, *Atmospheric Environment*, 2012, **54**, 272-276.

9. C. He, L. Morawska, H. Wang, R. Jayaratne, P. McGarry, G. Richard Johnson, T. Bostrom, J. Gonthier, S. Authemayou and G. Ayoko, Quantification of the relationship between fuser roller temperature and laser printer emissions, *Journal of Aerosol Science*, 2010, **41**, 523-530.

10. R. Bai, L. Zhang, Y. Liu, L. Meng, L. Wang, Y. Wu, W. Li, C. Ge, L. Le Guyader and C. Chen, Pulmonary responses to printer toner particles in mice after intratracheal instillation, *Toxicology Letters*, 2010, **199**, 288-300.

11. S. Pirela, I. Miousse, X. Lu, V. Castranova, T. Treye, Y. Qian, D. Bello, L. Kobzik, I. Koturbash and P. Demokritou, Effects of Laser Printer-Emitted Engineered Nanoparticles on Cytotoxicity, Chemokine Expression, Reactive Oxygen Species, DNA Methylation, and DNA Damage: A Comprehensive in Vitro Analysis in Human Small Airway Epithelial Cells, Macrophages, and Lymphoblasts, *Environmental Health Perspectives (Online)*, 2016, **124**, 210.

12. C. S.-J. Tsai, N. Shin, A. Castano, J. Khattak, A. M. Wilkerson and N. R. Lamport, A pilot study on particle emission from printer paper shredders, *Aerosol Science and Technology*, 2017, **51**, 57-68.

13. J. D. Sisler, S. V. Pirela, S. Friend, M. Farcas, D. Schwegler-Berry, A. Shvedova, V. Castranova, P. Demokritou and Y. Qian, Small airway epithelial cells exposure to printer-emitted engineered nanoparticles induces cellular effects on human microvascular endothelial cells in an alveolar-capillary co-culture model, *Nanotoxicology, 2015, Vol.9(6), p.769-779*, 2015, **9**, 769-779.

14. N. Kagi, Ultrafine Particle Contamination in Indoor Air and Emission from Printers, *Earozoru Kenkyu*, 2008, **23**, 252-256.

15. M. Scungio, T. Vitanza, L. Stabile, G. Buonanno and L. Morawska, Characterization of particle emission from laser printers, *Science of the Total Environment*, 2017, **586**, 623-630.

16. Z.-M. Wang, J. Wagner and S. Wall, Characterization of Laser Printer Nanoparticle and VOC Emissions, Formation Mechanisms, and Strategies to Reduce Airborne Exposures, *Aerosol Science and Technology*, 2011, **45**, 1060-1068.

17. M. Wensing, T. Salthammer, C. He, L. Morawska, T. Schripp and E. Uhde, Evaluation of Ultrafine Particle Emissions from Laser Printers Using Emission Test Chambers, *Environmental Science & Technology*, 2008, **42**, 4338-4343.

18. C. Tsai and D. Theisen, A sampler designed for nanoparticles and respirable particles with direct analysis feature, *Journal of Nanoparticle Research*, 2018, **20**, 1-14.

19. , 5443954 Immortalized non-tumorigenic human bronchial epithelial cell lines: Reddel Roger R; Ke Yang; Rhim Johng; Brash Douglas E; Su Robert; Lechner John F; Gerwin Brenda I; Harris Curtis C; Amstad Paul Camperdown, Australia assigned to The United States of America as represented by the Department of Health and Human Services, *Biotechnology Advances*, 1996, **14**, 514-514.

20. J. Lechner and M. LaVeck, A serum-free method for culturing normal human bronchial epithelial cells at clonal density, *Journal of tissue culture methods*, 1985, **9**, 43-48.

21. O. Sakamoto, A. Iwama, R. Amitani, T. Takehara, N. Yamaguchi, T. Yamamoto, K. Masuyama, T. Yamanaka, M. Ando and T. Suda, Role of macrophage-stimulating protein

and its receptor, RON tyrosine kinase, in ciliary motility, *The Journal of clinical investigation*, 1997, **99**, 701.

22. R. J. Hay, J. Caputo and M. Macy, *ATCC quality control methods for cell lines*, Amer Type Culture Collection, 1992.

23. J. Caputo, Biosafety procedures in cell culture, *Journal of tissue culture methods*, 1988, **11**, 223-227.

24. D. O. Fleming, J. H. Richardson, J. J. Tulis and D. Vesley, *Laboratory safety: principles and practices*, ASM Press Washington, DC, 1995.

25. J. R. Yankaskas, J. E. Haizlip, M. Conrad, D. Koval, E. Lazarowski, A. M. Paradiso, C. A. Rinehart, B. Sarkadi, R. Schlegel and R. C. Boucher, Papilloma virus immortalized tracheal epithelial cells retain a well-differentiated phenotype, *American Journal of Physiology-Cell Physiology*, 1993, **264**, C1219-C1230.

26. A. B. Alexander, Thermal properties of graphene and nanostructured carbon materials, *Nature Materials*, 2011, **10**, 569.

27. C. Monn, A. Fuchs, D. Högger, M. Junker, D. Kogelschatz, N. Roth and H. U. Wanner, Particulate matter less than 10 μm (PM 10) and fine particles less than 2.5 μm (PM 2.5): relationships between indoor, outdoor and personal concentrations, *Science of the Total Environment*, 1997, **208**, 15-21.

28. T. Osunsanya, G. Prescott and A. Seaton, Acute respiratory effects of particles: mass or number?, *Occupational and Environmental Medicine*, 2001, **58**, 154.

29. R. S. Osgood, B. L. Upham, P. R. Bushel, K. Velmurugan, K.-N. Xiong and A. K. Bauer, Secondhand Smoke-Prevalent Polycyclic Aromatic Hydrocarbon Binary Mixture-

Induced Specific Mitogenic and Pro-inflammatory Cell Signaling Events in Lung Epithelial Cells, *Toxicological Sciences*, 2017, **157**, 156-171.

30. L. Morawska, G. A. Ayoko, G. N. Bae, G. Buonanno, C. Y. H. Chao, S. Clifford, S. C. Fu, O. HäNninen, C. He, C. Isaxon, M. Mazaheri, T. Salthammer, M. S. Waring and A. Wierzbicka, Airborne particles in indoor environment of homes, schools, offices and aged care facilities: The main routes of exposure, *Environment International*, 2017, **108**, 75-83.

APPENDIX A: LIST OF TABLES

Table A1. ICP-MS individual sample results for printed and plain paper particle mixed media 39

Table A1. ICP-MS individual sample results for printed and plain paper particle mixed media

	Blank	Printed 1	Printed 2	Printed 3	Plain 1	Plain 2	Plain 3
	(µg/g)	(µg/g)	(µg/g)	(µg/g)	(µg/g)	(µg/g)	(µg/g)
Li	0	1.02	2.32	1.76	0.425	2.1	0
Be	0	0	0	0	0	0	0
B	13.3	0	0	0	20.7	0	0
Na	0	0	0	0	0	0	0
Mg	0	0	0	0	0	0	0
Al	16	42.6	33.6	32.5	140	311	269
Si	0	0	0	0	0	0	0
P	1480	4280	9280	8340	8270	7830	7440
S	0	0	0	0	0	0	0
Cl	0	0	0	0	0	0	0
K	0	0	0	0	0	0	0
Ca	335	4920	6990	6950	8900	10100	9240
Sc	1.54	1.32	0.145	0.146	0.425	0.421	0
Ti	5.8	5.27	10.2	9.07	9.06	10.9	8.29
V	7.17	12.4	10.3	7.32	13.6	11.5	12.3
Cr	23	53.7	45.9	38.8	59	64.1	53.6
Mn	0	1.02	1.16	1.46	2.97	1.26	0.714
Fe	0	318	642	372	919	560	308
Co	0	0.293	1.02	0.732	1.84	1.26	0.857
Ni	0.683	0	0	0	132	0	0
Cu	3.59	5.85	3.2	5.27	47	8.83	4
Zn	40.6	0	0	11.1	41.2	75.8	4.57
Ga	0	0.146	0.291	0	0.283	0.421	0.143
Ge	0	0	0	0	0	0	0
As	4.44	10.2	9.44	8.93	9.34	7.99	8.71
Se	0	0	0	0	0	0	0
Br	6.32	44.2	106	195	159	178	117
Rb	0	0.585	0.581	0.146	0.708	0	0.429
Sr	3.24	8.49	9.59	10.4	11.6	12.2	10.6
Y	0.171	0	0.145	0	0	0.14	0
Zr	0.512	0	0	0	0.283	0.421	0
Nb	9.39	3.66	0.581	1.17	0.425	0.701	1.71
Mo	0	0.293	0	0.439	1.27	0.981	0.571
Ru	0	0	0	0	0	0	0
Rh	0	0.146	0	0.293	0	1.12	0
Pd	0	0	0	0	0	0	0
Ag	0.171	0	0	0	0	0	0
Cd	0	0	0	0	0	0	0

In	0	0	0.145	0	0	0.14	0
Sn	1.02	0	0	0	0	0	0
Sb	0.512	0	0	0	0	0.28	0.143
Te	0	0	0	0	0	0	0
I	0	0	0	0	0	22.6	0
Cs	0.171	0	0.726	0	0.142	0	0
Ba	0	2.63	4.36	4.54	8.49	7.29	6.43
La	0.171	0	0	0	0	0	0
Ce	0	0	0	0	0	0.14	0
Pr	0	0	0	0	0	0	0
Nd	0.171	0	0	0	0	0	0
Sm	0	0	0	0	0	0	0
Eu	0	0	0	0	0	0	0
Gd	0	0	0	0	0	0	0
Tb	0	0	0.145	0	0	0	0
Dy	0	0	0	0	0	0	0
Ho	3.59	0.732	5.38	0	0.708	0.701	0
Er	0	0	0	0	0	0	0
Tm	7.17	0	7.55	0	0	0	0
Yb	0	0	0	0	0	0	0
Lu	8.88	0.732	6.83	1.46	0.708	2.94	1.43
Hf	0.512	0.293	0	0.146	0	0	0.143
Ta	248	92.6	32	52.8	32.5	38.1	68
W	0.341	0	0	0	0	0	0
Re	0	0	0.436	0	0	0	0
Os	0	0	0	0	0	0	0
Ir	0	0.146	0	0.732	0	1.12	0
Pt	0	0	0	0	0	0	0
Au	0	0	0	0	0	0	0
Hg	0	0.293	0	0	0	0	0
Tl	0	0.146	0.436	0	0	0	0.143
Pb	0.341	0	0	0	3.82	0	0
Bi	0.171	0	0	0	0.142	0	0
Th	2.22	0.585	0.145	0.146	0	0	0.286
U	0.854	0	2.32	1.46	0	0	0.714